Underwater magnetic target localization and characterization using a three-axis gradiometer

Eric Mersch*, Yann Yvinec*, Yves Dupont†, Xavier Neyt* and Pascal Druyts*

*CISS department
Royal Military Academy,
Brussels, Belgium
Email: eric.mersch@elec.rma.ac.be

†Belgian Navy,
Zeebrugge, Belgium

Abstract—**Magnetometers and magnetic gradiometers are commonly used to detect ferromagnetic targets. When the distance to the target is large compared to its size, the target can be modeled as a dipolar source and can then be characterized by a single vector: its magnetic moment. The estimation of the magnetic moment of the target can be used to reduce the false alarm rate. We consider a total-field three-axis gradiometer which measures the gradient of the magnitude of the magnetic field along three orthogonal axes. We show that for an ideal gradiometer, the inversion problem separates into two linear problems and can therefore be solved without any initial estimation of the parameters. Moreover, the method can be applied directly on the data gathered by the gradiometer, without any grid interpolation and in real time. For the considered gradiometer, a better estimation of the parameters can be obtained if the detailed geometry of the gradiometer (location of the magnetometers) is taken into account. We show that the method can be extended to magnetometers, vertical total-field gradiometers, horizontal total-field gradiometers and tensor gradiometers. Finally, we analyze the effect of various survey parameters (gradiometer altitude, inter-track distance and target magnetic moment) on the accuracy of the estimated parameters in the presence of noise (magnetic noise and error on the position of the gradiometer).**

I. Introduction

Detecting and localizing magnetic targets is useful in a large number of applications, such as unexploded ordnance detection [1], [2], underwater buried mine hunting [3], [4], underwater vessel detection [5], [6], archeologic survey [7], geologic prospecting [8] or biomedical applications [9], [10], [11]. When the distance between the target and the detector is large compared to the size of the target, The target can be modeled as a dipolar source characterized by its dipolar moment. Estimating the magnetic dipolar moment of the source makes it possible to classify the target [4] or to reduce the false alarm rate in the fields of underwater mine-hunting and unexploded ordnance cleanup [1], [2], [6]. In this work, we are considering the detection of sea mines on the seafloor or buried. Drifting mines or moored mines can be detected by other techniques [12], [13] and there is no need to use a gradiometer for those mines. For this reason, we focus on bottom mines. Nevertheless, the method presented here is not limited to this application.

Two main kinds of magnetic sensors are used to localize ferromagnetic targets: magnetometers and gradiometers. Magnetometers measure the local magnetic field. Some of them only measure the magnitude of the magnetic field (total-field magnetometers), other measure the field components (vector magnetometers). Gradiometers measure the gradient of the magnetic field and are therefore less sensitive to slowly varying magnetic fields (geologic or geomagnetic noise) than magnetometers. There exists two kinds of gradiometers: tensor gradiometers that measure the gradient of the magnetic field and total-field gradiometers that measure the gradient of the magnitude of the magnetic field. Some total-field gradiometers only measure one or two components of the gradient (vertical or horizontal total-field gradiometers). In this paper, we consider a three-axis total-field gradiometer, which measures all the three components of the gradient. It is composed of four total-field magnetometers separated by about 1 m. Combining the measurements taken by the magnetometers, an approximation of the gradient is obtained.

A common way to localize a magnetic target is to look at the maxima of the magnitude of the magnetic field gradient (sometimes called 3D analytic signal amplitude) [14], [15]. Most of the time, the maximum of this quantity is located approximately above the target. The depth of the target can be estimated from the width of the peak. However, this method is not accurate and it suffers from interpolation artifacts. Moreover, at low latitudes, up to four maxima can be observed for only one target, which can lead to misinterpretation. A more powerful technique to localize a dipolar source is the so-called Euler deconvolution [16], [17]. Three-axis gradiometers directly measure the quantities required for the Euler deconvolution [18]. No grid interpolation is needed. This allows one to estimate the target location directly from the raw data, giving more accurate results. The Euler deconvolution is a linear technique, it does not require any initial estimation of the parameters and it is free of local minima.

In this paper, we show that once the localization is done using the Euler deconvolution, the moment can be estimated by solving a second linear system. For the gradiometer considered, the Euler deconvolution is inaccurate, because the measurement is only an approximation of the gradient obtained from a finite difference of the magnetometers measurements and therefore a significant error appears on the estimated

position and in a second step, on the magnetic moment. Therefore, a second step in our inversion method is introduced, where the geometry of the gradiometer is taken into account.

We also study the influence of the principal survey parameters (gradiometer altitude and inter-track distance) on the estimated parameters in the presence of noise. We consider two sources of noise: the magnetic noise and the gradiometer position error. The analysis is done considering different magnetic moments covering a representative range for mines.

II. PROBLEM FORMULATION

Our objective is to determine the position $\mathbf{r}_s$ of a target and its magnetic moment $\mathbf{M}$ given the position $\mathbf{r}_g^\alpha$ of the gradiometer in the UTM reference frame, and the corresponding magnitudes of the magnetic field $|\mathbf{B}|_{star}^\alpha, |\mathbf{B}|_{port}^\alpha, |\mathbf{B}|_{down}^\alpha$ and $|\mathbf{B}|_{aft}^\alpha$ measured by the four magnetometers that compose the gradiometer, with $\alpha \in \{1, ..., N\}$ the index of the measurement. From the four magnetometers measurements, an estimation of the gradient is obtained:

$$\begin{pmatrix} \tilde{G}^{1,\alpha} \\ \tilde{G}^{2,\alpha} \\ \tilde{G}^{3,\alpha} \end{pmatrix} \equiv R^\alpha \begin{pmatrix} \frac{|\mathbf{B}|_{star}^\alpha - |\mathbf{B}|_{port}^\alpha}{L_{trans}} \\ \frac{(|\mathbf{B}|_{star}^\alpha + |\mathbf{B}|_{port}^\alpha) - 2|\mathbf{B}|_{aft}^\alpha}{2L_{long}} \\ \frac{(|\mathbf{B}|_{star}^\alpha + |\mathbf{B}|_{port}^\alpha) - 2|\mathbf{B}|_{down}^\alpha}{2L_{vert}} \end{pmatrix} \quad (1)$$

The $\sim$ symbol is introduced to make the difference between the finite difference estimation of the gradient and its true value:

$$G^{i,\alpha} = \frac{\partial |\mathbf{B}|^\alpha}{\partial r_g^{i,\alpha}}, i \in \{1,2,3\}$$

R^α is the rotation matrix to change from the reference frame fixed to the gradiometer to the UTM reference frame. The length L_{trans}, L_{long} and L_{vert} are explicated in Fig. 1, as well as the index "star","port","down" and "aft".
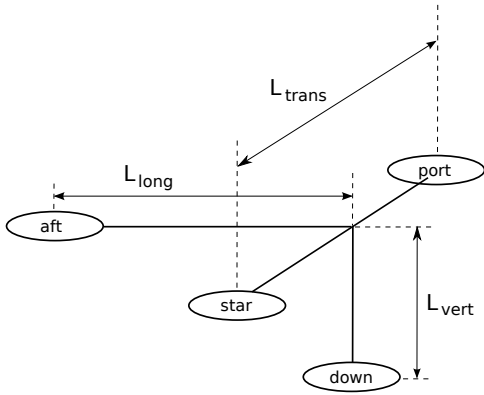

Fig. 1. Sketch of a three-axis total-field gradiometer showing the four magnetometerts "starboard", "port", "down" and "after". For the gradiometer considered, $L_{trans} = 1.5$ m, $L_{long} = 1.1$ m and $L_{vert} = 0.5$ m

The total field $\mathbf{B}$ has two contributions: the earth magnetic field $\mathbf{B}_e$ and the field $\mathbf{B}_s^\alpha$ due to the source target. If the distance between the target and the gradiometer is large compared to the size of the target, the field $\mathbf{B}_s^\alpha$ can be expressed as:

$$\mathbf{B}_s^\alpha = \frac{\mu_0}{4\pi |\mathbf{r}^\alpha|^5} \left(3\mathbf{r}^\alpha \left(\mathbf{r}^\alpha \cdot \mathbf{M} \right) - |\mathbf{r}^\alpha|^2 \mathbf{M} \right), \quad (2)$$

where μ_0 is the vacuum permeability and $\mathbf{r}^\alpha = \mathbf{r}_g^\alpha - \mathbf{r}_s$ is the vector pointing from the target to the gradiometer.

III. THE LINEAR MODEL

A function f is called homogeneous of degree d in $\mathbf{r}$ if

$$f(\lambda \mathbf{r}) = \lambda^d f(\mathbf{r})$$

for all $\lambda > 0$. A remarkable property of such a function is that it fulfills the Euler's homogeneity equation, which reads [19]:

$$\mathbf{r} \cdot \nabla f(\mathbf{r}) = d\, f(\mathbf{r})$$

Let define the magnetic anomaly T^α as:

$$T^\alpha \equiv |\mathbf{B}|^\alpha - |\mathbf{B}_e| \quad (3)$$

If $|\mathbf{B}_s| << |\mathbf{B}_e|$,

$$T^\alpha \approx \mathbf{B}_s^\alpha \cdot \hat{\mathbf{B}}_e, \quad (4)$$

where $\hat{\mathbf{B}}_e \equiv \frac{\mathbf{B}_e}{|\mathbf{B}_e|}$ is the unit vector in the direction of $\mathbf{B}_e$. According to (2), the components of $\mathbf{B}_s^\alpha$ are homogeneous functions of degree -3 in $\mathbf{r}^\alpha$. Therefore, according to (4), T^α is also a homogeneous function of degree -3 in $\mathbf{r}^\alpha$. Under these conditions, the Euler's homogeneity equation is fulfilled for T^α. It reads:

$$(r^{1,\alpha})G^{1,\alpha} + (r^{2,\alpha})G^{2,\alpha} + (r^{3,\alpha})G^{3,\alpha} = -3T^\alpha,$$

where the true gradient $G^{i,\alpha}$ and can be approximated by the measured gradient $\tilde{G}^{i,\alpha}$. This system of equations was first derived by Thompson [16]. It can be rewritten in a matrix form:

$$X\theta = Y,$$

with

$$X = \begin{pmatrix} \tilde{G}^{1,1} & \tilde{G}^{2,1} & \tilde{G}^{3,1} & 3 \\ \tilde{G}^{1,2} & \tilde{G}^{2,2} & \tilde{G}^{3,2} & 3 \\ \vdots & \vdots & \vdots & \vdots \\ \tilde{G}^{1,N} & \tilde{G}^{2,N} & \tilde{G}^{3,N} & 3 \end{pmatrix},$$

$$\theta = \begin{pmatrix} r_s^1 \\ r_s^2 \\ r_s^3 \\ |\mathbf{B}_e| \end{pmatrix},$$

$$Y = \begin{pmatrix} 3|\mathbf{B}|^1 + r_g^{1,1}\tilde{G}^{1,1} + r_g^{2,1}\tilde{G}^{2,1} + r_g^{3,1}\tilde{G}^{3,1} \\ 3|\mathbf{B}|^2 + r_g^{1,2}\tilde{G}^{1,2} + r_g^{2,2}\tilde{G}^{2,2} + r_g^{3,2}\tilde{G}^{3,2} \\ \vdots \\ 3|\mathbf{B}|^N + r_g^{1,N}\tilde{G}^{1,N} + r_g^{2,N}\tilde{G}^{2,N} + r_g^{3,N}\tilde{G}^{3,N} \end{pmatrix}$$

If $N > 4$, this forms an over-determined linear system of equations for which the least mean square (LMS) solution is:

$$\theta = (X^T X)^{-1} X^T Y \quad (5)$$

Equation (5) provides an expression for the estimated target position. Once this position is known, according to (2) and (4), T^α becomes a linear function of M^i. As the gradient is a linear operator, the same holds for the gradient $G^{i,\alpha}$. Indeed, differentiating (4) leads to:

$$
\begin{aligned}
G^{i,\alpha} = {} & \frac{\mu_0}{4\pi}\left(-\frac{5r^{i,\alpha}}{|\mathbf{r}^\alpha|^7}\right) 3\mathbf{M}\cdot\left(\mathbf{r}^\alpha(\hat{\mathbf{B}}_e\cdot\mathbf{r}^\alpha)-\hat{\mathbf{B}}_e|\mathbf{r}^\alpha|^2\right)\\
& +\frac{\mu_0}{4\pi|\mathbf{r}^\alpha|^5}\left(3\hat{B}_e^i\left(\mathbf{M}\cdot\mathbf{r}^\alpha\right)-2r^{i,\alpha}\left(\mathbf{M}\cdot\hat{\mathbf{B}}_e\right)\right)\\
& +\frac{\mu_0}{4\pi|\mathbf{r}^\alpha|^5}3M^i\left(\mathbf{r}^\alpha\cdot\hat{\mathbf{B}}_e\right)
\end{aligned}\tag{6}
$$

This expression is linear in M^i. It can therefore be estimated by the linear least mean square method assuming that $\tilde{G}^{i,\alpha} = G^{i,\alpha}$.

The motivation for using the gradient $G^{i,\alpha}$ in stead of the magnitude $|\mathbf{B}|^i$ of the magnetic field is that we don't know $|\mathbf{B}_e|$ with a sufficient accuracy. Using (3) and (4) leads to a bad estimation of the parameters because T^α is the difference between two nearly equal numbers. The problem disappears when using (6) which only depends on the direction $\hat{B}_e^i$.

IV. The nonlinear refinement

In the previous section, we described a method to retrieve the position and the magnetic moment of a target from a gradiometer survey. It was based on three assumptions:

- The field due to the target is dipolar.

- The field due to the target is small compared to the earth magnetic field.

- The gradiometer gives a measure of the true gradient.

The two first assumptions are usually fulfilled in practice. However, strictly speaking, the considered gradiometer only provides an approximation of the gradient by measuring the magnitude of the total magnetic field at four different locations. This approximation is accurate if the distance to the target is large compared to the size of the gradiometer. The size of the gradiometer considered is about 1 m and the distance to the target can be as small as 6 m. In those conditions, the accuracy of the estimated parameters may be poor. Therefore, to increase the estimation accuracy, we introduce a second step in the parameter estimation. In that step, the detailed gradiometer geometry is taken into account by solving the system of equations (1). The position and the magnetic moment are refined simultaneously, leading to a nonlinear problem. This problem is solved by the Levenberg-Marquardt algorithm, which requires initial values for the parameters $\mathbf{r_s}$ and $\mathbf{M}$. These initial values are computed assuming that the gradiometer measures the true gradient and by solving the two successive linear methods described in section III.

V. Discussion

In this section, we compare the approach presented in sections III and IV to more traditional map production. This comparison in done using synthetic data. Fig. 2 shows the contour map of the gradient magnitude. It also shows the real position of the target, the positions estimated with the Euler method and the nonlinear method. The analysis of the map gives inacurate results: due to the low latitude, several maxima are visible. The Euler method gives better results. However, as expected, the most accurate results are given by the nonlinear method. This method has also the advantage over map interpretation that it provides an estimation of the depth and the magnetic moment of the target. Further, and contrary to other approaches [2], [4], our method works regardless of the latitude and of the dipole orientation and can be applied in real-time.
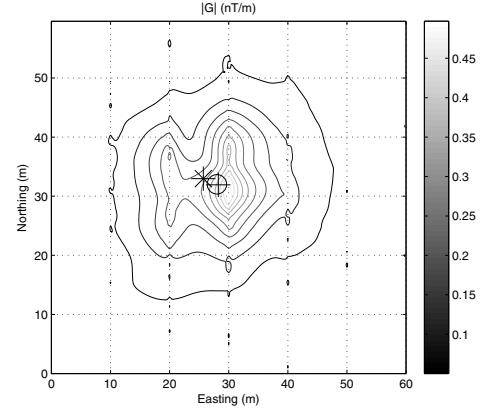

Fig. 2. Contour map of the gradient magnitude with the actual position of the target (circle) and the position found with the Euler method (star) and the nonlinear method (cross) described in sections III and IV. The map exhibits several maxima for only one target, as a consequence of the low latitude. The most accurate method is the nonlinear one.

We considered here a three-axis gradiometer. However, the linear method could also be applied to tensor gradiometers survey since there exist relations linking the total-field gradient to the magnetic gradient tensor. Indeed, taking the gradient of both members of (4) yields to:

$$
G^{i,\alpha} = \sum_{j=1}^{3} g^{i,j,\alpha}\hat{B}_e^j
$$

This expression directly gives the total-field gradient components $G^{i,\alpha}$ in terms of tensor gradient components $g^{i,j,\alpha}$. The linear method could be applied to vertical gradiometers and horizontal gradiometers as well, since there exist relations that allow one to compute an approximation of the vertical gradient in terms of horizontal ones and reciprocally [20]. However, this means that some grid interpolation needs to be done. It is then not possible to apply the algorithm in real time for these sensors. Similarly, one can derive the horizontal gradients from magnetometers survey, it is then possible to apply the linear method to magnetometers data. In principle, the linear method could help to find initial values before applying a refining method adapted to the kind of sensor considered.

VI. Effect of the survey parameters on the estimated parameters

To assess the effect of survey parameters on the accuracy of the estimated parameters, some numerical simulations were

performed for various scenarios. We first compare the linear and the nonlinear method in the absence of noise for various gradiometer altitudes. Then, we analyze the effect of the gradiometer altitude and the inter-track distance on the accuracy of the estimated parameters for various magnetic moment of the target in the presence of noise.

In Fig. 3, the linear and the nonlinear methods are compared for ideal conditions (no noise). The following scenario is considered. The earth magnetic field magnitude is of $48769\,\text{nT}$, its delination is of $-0.136°$ and its inclination is of $66.579°$. The gradiometer trajectory is a single south-north track of $60\,\text{m}$ above a target of magnetic moment $M^1 = M^2 = M^3 = \frac{50}{\sqrt{3}}\,\text{Am}^2$. The gradiometer speed is 2 kts and the sampling rate is $1\,\text{Hz}$. This corresponds to a measurement every $1\,\text{m}$ approximately. For gradiometer altitudes between 4 to $22\,\text{m}$, we compare the estimation errors on the magnetic moment and on the position for both linear and nonlinear methods. More precisely, we define the relative position error as $\frac{|\mathbf{r}_s - \tilde{\mathbf{r}}_s|}{r^3}$ and the relative moment error as $\frac{|\mathbf{M}| - |\tilde{\mathbf{M}}|}{|\mathbf{M}|}$, with $\mathbf{r}_s$ the true position of the target, $\tilde{\mathbf{r}}_s$ the estimated position of the target, r^3 the altitude of the gradiometer, $\mathbf{M}$ the true magnetic moment and $\tilde{\mathbf{M}}$ the estimated magnetic moment.

As expected, the nonlinear method gives perfect results regardless of the altitude. In contrast, the linear method is inaccurate, especially at low altitudes, because the gradiometer only provides an inaccurate estimation of the gradient ($\tilde{G}^{i,\alpha} \approx G^{i,\alpha}$).
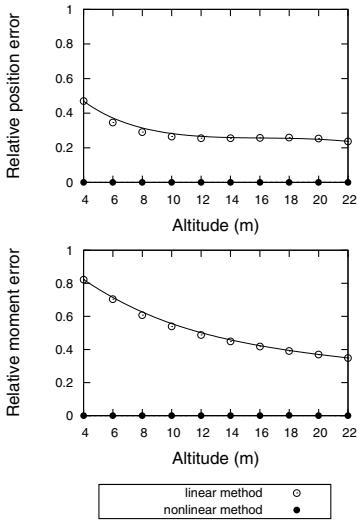
Fig. 3. Relative position and moment error as a function of the altitude of the gradiometer for the linear and the nonlinear methods in the absence of noise.

In Fig. 4, the effect of the gradiometer altitude and the target magnetic moment on the accuracy of the estimated parameters is investigated in the presence of noise for the nonlinear method. Three sources of noise are considered: the gradiometer position error, the geomagnetic noise and the intrinsic noise of the magnetometers. The gradiometer position error is modeled as an uncorrelated Gaussian noise with a standard deviation of $0.2\,\text{m}$. The geomagnetic noise is modeled as a correlated noise applied simultaneously on

each magnetometer. The amplitude spectral density of this noise scales as $f^{-5/4}$ and has a mean of $0.03\,\text{nT Hz}^{-1/2}$ at $1\,\text{Hz}$, as observed by Beard [21]. The intrinsic noise of the magnetometers is modeled as an uncorrelated Gaussian noise with a standard deviation of $0.01\,\text{nT}$. We don't consider any error on the orientation angles of the gradiometer because they can be measured during the survey and because adding a noise on these angles has a negligible influence on the estimated parameters. We don't consider any geologic noise in this paper neither any swell induced magnetic noise. Each point is the mean error calculated on 200 runs. Since only 200 runs were performed, there subsists a noise on the error values, therefore, we used Bézier curves as guides for the eye.
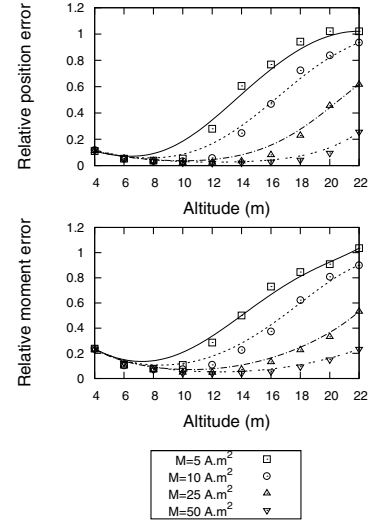
Fig. 4. Relative position and moment error as a function of the gradiometer altitude for the nonlinear method with magnetic noise and noise on the gradiometer position. Two sources of magnetic noise are considered: the intrinsic noise of the magnetometers and the geomagnetic noise. The results are shown for four different values of the magnetic moment. The track passes just above the target.

At small altitudes, gradiometer position error induces errors on the estimated parameters regardless of the magnetic moment. Actually, without magnetic noise, the closer the gradiometer is to the dipolar source, the greater the error on the estimated parameters is. At high altitudes, the magnetic noise induces errors on the estimated parameters. Indeed, the signal to noise ratio decreases because the signal from the dipolar source decreases with the distance to the source. At high altitudes, the error on the estimated parameters decreases with increasing magnetic moment. This is expected because the signal to noise ratio increases with the magnetic moment. To get an optimal parameter estimation, an altitude between $6\,\text{m}$ and $10\,\text{m}$ should be chosen for the scenario considered. This guaranties that the magnetic moment relative error remains below $20\,\%$ and that the corresponding mean absolute position error is smaller than $0.5\,\text{m}$ for all the magnetic moment values.

Finally, the effect of the inter-track distance on the accuracy of the estimated parameters is investigated in Fig. 5. In practice, the target can be located anywhere between the tracks, we therefore consider the worst case, where the target is located in the middle of two tracks. In other words, we consider one single track and we fix the horizontal distance

between the track and the target to $L/2$, where L is the inter-track distance. We fix the gradiometer altitude to 6 m, since we have seen that this is the minimal acceptable altitude to guarantee that the relatve moment error remains below 20%. By fixing the altitude to 6 m, we are sure that the gradiometer remains at a sufficient altitude even if it passes above the target. Fig. 5 shows the effect of the inter-track distance on the estimated position and magnetic moment errors in the presence of noise and for different values of the magnetic moment. The characteristics of the noise are the same as for Fig. 4.
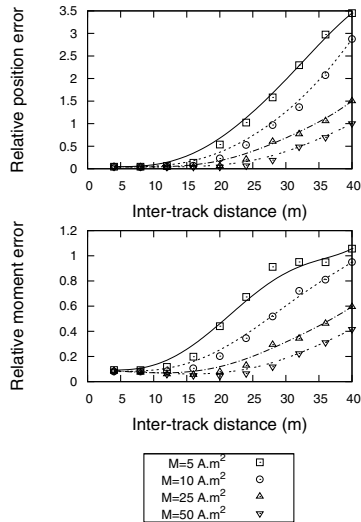

Fig. 5. Relative position and moment error as a function of the inter-track distance for the nonlinear method with magnetic noise and noise on the gradiometer position. Two sources of magnetic noise are considered: the intrinsic noise of the magnetometers and the geomagnetic noise. The results are shown for four different values of the magnetic moment.

To optimize the survey time, the inter-track distance should be chosen as large as possible for a given requirement on the estimated parameter accuracy. If a maximal error of 20% on the magnetic moment is accepted, an inter-track distance up to 16 m can be chosen for targets of magnetic moments as small as 5 Am^2 and for the noise parameters considered. This corresponds to a mean absolute position error of 0.8 m.

VII. CONCLUSION

A new inversion method allowing the estimation of target position, depth and magnetic moment from a gradiometer survey is presented. The method has been implemented and tested for three-axis gradiometers but generalization to other magnetic sensor types (magnetometers, vertical and horizontal total-field gradiometers, tensor gradiometers) is possible. The estimation can be done using measurements on a single track and does not rely on grid interpolation. This avoids artifacts that impair other methods using map generation. Moreover, the presented method works regardless of the latitude and of the magnetic moment orientation.

The inversion is performed in two steps: a linear inversion followed by a nonlinear refinement. In the first step, the target position and depth are retrieved using Euler deconvolution. Then, the target magnetic moment is estimated by solving a

linear system. The Euler deconvolution is based on the assumption that the sensor measures the true gradients. However, the sensor actually computes an estimation of the gradient from a finite difference of two magnetometer measurements and the assumption underlying Euler deconvolution is therefore only accurate when the distance to the target is large when compared to the distance between two magnetometers. This is not the case for the marine underwater buried sea mine hunting scenario considered.

As explained, the first step is linear. It is therefore fast, doesn't require any initial parameter estimation and is free of local minima. The accuracy of the estimated parameters is however limited because the underlying assumption is not very justified. We therefore introduce a second step in which the gradiometer true geometry is taken into account. This requires a non-linear estimation for which the output of the first step is used as initial values for the parameters. We show that the second nonlinear step significantly improves the accuracy of the estimated parameters.

To support the definition of operational procedures, the accuracy of the estimated parameters was evaluated as a function of two major survey parameters: the sensor altitude and the inter-track distance. This was done on synthetic data, taking into account the noise on the gradiometer position as well as two important sources of magnetic noise: the geomagnetic noise and the intrinsic noise of the magnetometers. It appeared that, for the scenario considered (sensor altitude: 6 m, target magnetic moment of 5 Am^2, maximum target moment error of 20% and for a track above the mine), the optimal sensor altitude is between 6 m and 10 m. Once the optimal altitude has been chosen, the inter-track distance should be optimized since it has a large impact on the survey duration. For the scenario considered, the optimal inter-track distance was found to be 16 m. Obviously, the optimal survey parameters are functions of the specificities of a given mission. The approach presented allows to objectively define the survey parameters and this may significantly improve the mission efficiency.

ACKNOWLEDGMENT

REFERENCES

[1] S. D. Billings. *Discrimination and classification of buried unexploded ordnance using magnetometry.* IEEE Transactions on Geoscience and Remote Sensing, **42**, 6, 1241 2004.

[2] S. D. Billings and F. Herrmann. *Automatic detection of position and depth of potential UXO using continuous transforms.* SPIE Conference on Detection and Remediation Technologies for Mines and Minelike Targets, (Orlando, USA), 2003.

[3] G. L. Allena, G. Sulzberger, J. T. Bono, J. S. Pray and T. R. Clem. *Initial evaluation of the new real-time tracking gradiometer designed for small unmanned underwater vehicles.* Proceedings of MTS/IEEE OCEANS, 1956 2005.

[4] Y. Yvinec, P. Druyts, and Y. Dupont. *Detection and Classification of Underwater Targets by Magnetic Gradiometry.* Proceedings of International Conference on Underwater Remote Sensing 2012, Brest, France, 2012.

[5] A. Sheinker, L. Frumkis, B. Ginzburg, N. Salomonski and B.-Z. Kaplan. *Magnetic anomaly detection using a three-axis magnetometer.* IEEE Trans. Magn., **45**, 1, 160 2009.

[6] A. Sheinker, B. Lerner, N. Salomonski, B. Ginzburg, L. Frumkis and B.-Z. Kaplan. *Localisation and magnetic moment estimation of ferromagnetic target by simulated annealing.* Meas. Sci. Technol. **18** (2007), 3451 2007.

[7] V. Schultze, A. Chwala, R. Stolz, M. Schulz, S. Linzen, H.-G. Meyer, T. Schüler. *A superconducting quantum interference device system for geomagnetic archaeometry.* Archaeological Prospection 14(**3**), 226 2007

[8] T. Rabeh, T. Abdallatif, M. Mekkawi, A. Khalil and A. El-Emam. *Magnetic data interpretation and depth estimation constraints : a correlative study on magnetometer and gradiometer data.* NRIAG Journal of Geophysics, Special Issue, 185 2008

[9] W. Yang, C. Hu, M. Q.-H. Meng, S. Song, and H. Dai. *A six-dimensional magnetic localization algorithm for rectangular magnet objective based on a particle swarm optimizer.* IEEE Trans. Magn., **45**, 8,3092 2009

[10] C. Hu, M. Q.-H. Meng, and M. Mandal. *A linear algorithm for tracing magnet position and orientation by using three-axis magnetic sensors.* IEEE Trans. Magn., **43**, 12, 4096 2007

[11] J. A. Baldoni and B. B. Yellen. *Magnetic tracking system: Monitoring heart valve prostheses.* IEEE Trans. Magn., **43**, 6, 2430 2007

[12] A. Borghgraef, O. Barnich, F. D. Lapierre, M. Van Droogenbroeck, W. Philips and M. Acheroy. *An Evaluation of Pixel-Based Methods for the Detection of Floating Objects on the Sea Surface.* EURASIP J. Adv. Sig. Proc 01/2010 2010

[13] S. D. Ladner, R. Arnone, J. Jolliff, B. Casey and K. Matulewski. *Forecasting the Ocean Optical Environment in Support of Navy Mine Warfare Operations.* Proc. of SPIE **8372** 2012

[14] X. Li. *Understanding 3D analytic signal amplitude.* Geophysics, **71**, 2, L13 2006

[15] W. E. Roest, J. Verhoef and M. Pilkington. *Magnetic interpretation using the 3-D analytic signal.* Geophysics, **57**, 116 1992

[16] D. T. Thompson. *EULDPH: A new technique for making computer-assisted depth estimates from magnetic data.* Geophys. **47**, 31 1982

[17] A. B. Reid, J. M. Allsop, H. Granser, A. J. Millet and I. W. Somerton. *Magnetic interpretation in three dimensions using Euler deconvolution.* Geophysics **55**, 1, 80 1990.

[18] X. Changhan, L. Shengdao and Z. Guo-hua. *Real-time localization of a magnetic object with total field data.* Automation Congress, 2008. WAC 2008. World 2008

[19] R. Adams and C. Essex. *Calculus: A Complete Course.* Pearson Canada, 2013.

[20] J. B. Nelson. *An alternate derivation of the three-dimensional Hilbert transform relations from first principles.* Geophysics, **51**, 1014 1986

[21] M. W. Beard. *Power spectra of geomagnetic fluctuations between 0.02 and 20 Hz.* NAVAL POSTGRADUATE SCHOOL MONTEREY CA, 1981